HHS Public Access

Author manuscript

Strahlenther Onkol. Author manuscript; available in PMC 2018 May 01.

Published in final edited form as:

Strahlenther Onkol. 2017 May ; 193(5): 410–418. doi:10.1007/s00066-017-1114-0.

Framework for radiation pneumonitis risk stratification based on anatomic and perfused lung dosimetry

Gurleen Dhami, MD[1], **Jing Zeng, MD**[1], **Hubert J. Vesselle, PhD, MD**[2], **Paul E. Kinahan, PhD**[2], **Robert S. Miyaoka, PhD**[2], **Shilpen A. Patel, MD**[1], **Ramesh Rengan, MD, PhD**[1], and **Stephen R. Bowen, PhD**[1,2]

[1]Department of Radiation Oncology, University of Washington School of Medicine, Seattle, WA 98195, USA

[2]Department of Radiology, University of Washington School of Medicine, Seattle, WA 98195, USA

Abstract

Purpose—To design and apply a framework for predicting symptomatic radiation pneumonitis in patients undergoing thoracic radiation, using both pre-treatment anatomic and perfused lung dose-volume parameters.

Material and Methods—Radiation treatment planning CT scans were co-registered with pre-treatment [^{99m}Tc]MAA perfusion SPECT/CT scans of 20 patients who underwent definitive thoracic radiation. Clinical radiation pneumonitis was defined as grade ≥ 2 using the CTCAE v4 grading system. Anatomic lung dose-volume parameters were collected from the treatment planning scans. Perfusion dose-volume parameters were calculated from pre-treatment SPECT/CT scans. Equivalent doses in 2 Gy per fraction were calculated in the lung to account for differences in treatment regimens and spatial variations in lung dose ($EQD2_{lung}$).

Results—Anatomic lung dosimetric parameters (MLD) and functional lung dosimetric parameters ($pMLD_{70\%}$) were identified as candidate predictors of grade ≥ 2 radiation pneumonitis (AUC>0.93, p<0.01). Pairing of an anatomic and functional dosimetric parameter (e.g. MLD and $pMLD_{70\%}$) may further improve prediction accuracy. Not all individuals with high anatomic lung dose (MLD>13.6 Gy$EQD2_{lung}$, 19.3 Gy for patients receiving 60 Gy in 30 fractions) went on to develop radiation pneumonitis, but those who also had high mean dose to perfused lung ($pMLD_{70\%}$>13.3 GyEQD2) all went on to develop radiation pneumonitis.

Conclusions—A framework for extracting perfused lung SPECT/CT parameters under standardized treatment position acquisition and image co-registration was developed. Its preliminary application revealed differences between anatomic and perfused lung dosimetry in this limited patient cohort. The addition of perfused lung parameters may help risk stratify patients for

Corresponding author address: Stephen R. Bowen, Ph.D., Assistant Professor, Departments of Radiation Oncology and Radiology, University of Washington School of Medicine, 1959 NE Pacific Street Box #356043, Seattle, WA 98195, 206.543.6559, srbowen@uw.edu.

Conflicts of interest

Dr. Bowen declares grants from NIH/NCI and the Radiological Society of North America during the conduct of the study. Dr. Zeng declares grants from NIH/NCI. Drs. Dhami, Patel and Rengan declare no conflicts of interest. Drs. Miyaoka and Vesselle declare grants from Philips Healthcare outside of the submitted work. Dr. Kinahan declares a commercial interest as a co-founder of PET/X, LLC, and grants from GE Healthcare outside of the submitted work.

radiation pneumonitis, especially in treatment plans with high anatomic mean lung dose. Further investigation is warranted to validate our results in a larger patient population.

Keywords

radiation pneumonitis; lung perfusion; risk stratification

Introduction

Many patients undergoing thoracic radiotherapy have compromised baseline pulmonary function. Assessing risk of radiation-induced pulmonary toxicity heavily relies on CT-based lung dose-volume parameters. Radiation pneumonitis after definitive doses is associated with significant morbidity with moderate to severe pulmonary toxicity of approximately 10–30% and fatal toxicity in 2% of these patients [1,2]. Anatomic lung constraints have been explored in the literature and are predictive for lung injury, most notably volume of lung receiving >20 Gy (V_{20Gy}) and mean lung dose (MLD), as well as additional risk factors, including elevated dose rate, concurrent carboplatin/paclitaxel and older age [2–5]. However, the predictive values of anatomic constraints are suboptimal, and even with V_{20Gy}<20%, there is still about an 18% chance of ≥grade 2 pulmonary toxicity [2].

Single photon emission computed tomography (SPECT) is a sensitive modality for measuring regional lung physiological processes. Pretreatment SPECT imaging has shown perfusion defects at the tumor site and adjacent tissue [6]. Perfusion has been shown to be a sensitive metric for assessing radiation induced-lung injury [7]. Data from Duke University [6,8], the Netherlands Cancer Institute (NKI) [9], and the Princess Margaret Hospital (PMH) have suggested a dose-response relationship between regional perfusion changes on SPECT imaging and dose delivered, association between a decline PFT values and changes in regional perfusion variables post-treatment, and correlation between perfusion changes post-treatment and risk of later developing radiation pneumonitis [10]. These studies have provided useful functional metrics but have not been able to produce functional lung constraints that can replace the anatomic parameters currently in use.

SPECT imaging comes with limitations of lower spatial resolution, quantitative uncertainties such as spatially-varying attenuation, scatter, detector response, and time duration for image acquisition [11]. Integration of CT with SPECT provides data for attenuation and scatter correction, but primarily increases the specificity of findings through spatially co-localized anatomical data with physiologic uptake [12]. Technical advances in scatter estimation and spatial resolution recovery have increased the potential for quantitative imaging with SPECT/CT [13–15]. This has increased the utility of incorporating SPECT/CT into the planning and assessment of radiation therapy.

The purpose of this study was to develop a framework for testing perfused lung dosimetric parameters defined on modern [^{99m}Tc]MAA SPECT/CT treatment planning imaging in thoracic cancer patients for correlation to incidence of radiation treatment-induced pneumonitis. We incorporated SPECT/CT acquisition and reconstruction protocols with data corrections, along with high spatial alignment accuracy through scanning of patients immobilized in treatment position, for improved parameter estimation. Similar to other

published studies, we assessed associations between varying levels of functional lung dose and volume parameters to the incidence of clinical radiation pneumonitis [9,16,17]. However, we extended this work by evaluating a range of dose volumes and perfusion mean lung dose parameters on modern SPECT/CT, while seeking complementarity between anatomic and functional image features. Additionally, we accounted for differences in radiation therapy fractionation, as well as regional variation in lung tissue fractional dose, in our patient cohort by converting physical radiation dose distributions to equivalent 2 Gy per fraction equivalent dose distributions.

Methods and Materials

Patient Characteristics

The framework was applied to a cohort of patients with the approval of the XXX IRB. Approximately half the patients were enrolled on a prospective trial looking at SPECT/CT changes in patients receiving radiation to the lungs (clinical trials.gov identifier XXX). All patients receiving definitive thoracic radiation from 2013 to 2015 with either a lung primary or metastatic disease to the lungs and a pre-treatment perfusion [^{99m}Tc]MAA SPECT/CT were included. The clinical characteristics of the patients were collected and are further described in in Table 1. Pulmonary morbidity was graded by the National Cancer Institute's Common Terminology Criteria for Adverse Events version 4 for pneumonitis. Patients were dichotomized for pulmonary toxicity based on presence or absence of grade ≥ 2 pneumonitis, defined by CTCAE v4 as the clinical indication for prednisone administration. All patients had >6 months follow up. Patients were typically seen at least once every 3 months, with toxicity assessment at each visit. Complete details of patient characteristics can be found in Supplemental Table 1.

Image acquisition and treatment planning

Patients were simulated for radiation therapy with a respiratory-correlated 4DCT simulation scan, which required abdominal compression for those receiving SBRT. The gross tumor volume (GTV) was delineated on individual phases of the 4DCT. The clinical target volume (CTV) and planning target volume (PTV) were constructed based on microscopic disease extension, respiratory motion, and setup uncertainties following ICRU83. CTV margins were typically 5–8 mm (0 mm for SBRT), and PTV margins were 5–10 mm. Target volumes were constructed following a similar paradigm for all radiation treatment modalities. Radiation therapy plans were generated in Pinnacle™ (Philips Healthcare) for photon therapy or CMS Xio™ (Elekta Inc.) for uniform scanning proton therapy, and radiation dose was calculated exclusively on the phase-averaged 4DCT images. Beam-specific proton range uncertainties of 2.5% and 2 mm, respectively, were incorporated as treatment planning structures to maintain similar target coverage as photon plans. Planned dose optimization incorporated only conventional anatomic dose objectives, including limits on mean lung dose and lung volume fraction receiving higher than 20 Gy (V_{20Gy}). Functional lung imaging data from MAA SPECT/CT was not incorporated into treatment planning constraints.

Patients underwent baseline pre-treatment lung perfusion exams using the same immobilization devices as the treatment simulation 4DCT, including indexing of an abdominal compression plate where indicated. Perfusion [^{99m}Tc]MAA SPECT scans were acquired on a dual-head SPECT/CT camera (Precedence system, Philips Healthcare) following an intravenous infusion of 5 mCi of Tc99m-MAA. The SPECT acquisition protocol consisted of 12 seconds per angular projection and 64 total angles over 180 degrees (i.e. 128 projections over 360 degrees) following an elliptical detector trajectory. MAA SPECT images were reconstructed with the Astonish™ (Philips Healthcare) OSEM algorithm (2 iterations, 16 subsets, 10 mm cutoff Hanning filter), which incorporates iterative geometric collimator resolution recovery along with model-based scatter and CT-based attenuation correction, onto grids of isotropic 4.64 mm voxels. Helical CT scans were acquired during the same imaging session either at end-exhale following voluntary breath hold for the majority of patients, or free-breathing conditions for SBRT patients under abdominal compression. These conditions were chosen to maximize signal recovery in the lower lung lobes due to attenuation, to capture the diaphragm at its most likely end-exhale position for most patients, and finally to mimic patient setup conditions present during the treatment simulation scans.

Image and dosimetric analysis

The treatment planning 4DCT phase-averaged image, corresponding 4DCT 10 phase-binned images, and registered radiation dose matrix were DICOM transferred to MIM 6.5™ (MIM Software Inc. Cleveland, OH) for image processing. Free-breathing helical CT scans used for SPECT attenuation and scatter correction were rigidly co-registered with the respective phase-averaged 4DCT images, while end-exhale helical CT were co-registered with the appropriate end-exhale phase 4DCT. Registration accuracy was evaluated over the total lung, with particular attention given to regions near the tumor, regions with high perfusion, and regions with high anatomic reproducibility where indicated such as the spine, mediastinum, and great vessels. Rigid alignment of MAA SPECT images was automatically applied through shared DICOM coordinates with the helical CTAC, bringing them into spatial alignment with both planning CT and radiation dose grids. Radiation dose distributions in the lung were converted to biologically equivalent voxel dose distributions in 2 Gy fraction sizes ($EQD2_{lung}$) using the linear-quadratic model for a clinical endpoint of pneumonitis (α/β = 3 Gy) [3,18]. This methodology accounted for differences in treatment regimens as well as spatial variations in lung fractional dose.

Anatomic regions of interest included total lung minus GTV (TL-GTV), and functional lung regions of interest included threshold percentages of maximum perfusion (5%–95%, 5% increments) within TL-GTV, to generate perfusion pTL-$GTV_{xx\%}$. Examples of pTL-$GTV_{25\%}$, pTL-$GTV_{50\%}$, and pTL-$GTV_{75\%}$ are depicted in Figure 1. From these regions, anatomic dosimetric parameters were extracted: mean lung dose (MLD) and % TL-GTV volume receiving above absolute doses in 5 Gy $EQD2_{lung}$ increments ($V_{5\text{-}70GyEQD2}$). Physical doses and biologically equivalent doses to anatomical structures were reported to facilitate comparison to prior studies. Similar to anatomic dose volumes such as $V_{20GyEQD2}$, functional dose volume parameters included % TL-GTV perfusion, calculated as a ratio of total MAA SPECT counts above absolute dose thresholds ($pV_{5\text{-}70GyEQD2}$). We also

calculated mean dose to perfused lung regions defined by MAA SPECT count thresholds ($pMLD_{5–95\%}$).

Statistical analysis

Receiver operating characteristic (ROC) curves tested the prediction accuracy of mean lung dose (MLD), mean perfused lung dose ($pMLD_{5\%–95\%}$), anatomic dose-volume parameters ($V_{5\text{-}70GyEQD2}$), and dose-perfused volume parameters ($pV_{5\text{-}70GyEQD2}$) for association with grade 2 or higher (G2+) pneumonitis status. Parameters were considered statistically significant if the two-tailed asymptotic p-value for the area under the curve (AUC, null hypothesis AUC = 0.5) was less than 0.01, which took into account multiple testing adjustment with false discovery rate (FDR) of 5%. When testing a total of 48 free parameters in this investigation, the threshold of significance equates to the FDR-corrected p-value of 0.03 using the Benjamini-Hochberg method [19]. While not as conservative an adjustment as Bonferroni's correction of familywise error rate, this threshold of significance balanced mitigation of false positive discoveries while maintaining statistical power in this small cohort to identify candidate predictors of pneumonitis. Standard errors in AUC estimates, defined relative to 95% confidence intervals, were reported. Cutoff values of mean lung dose (MLD) and perfused mean lung dose (pMLD) were estimated that balanced sensitivity and specificity for classifying patients with/without G2+ pneumonitis. Bivariate thresholds were empirically estimated through observation of pairs of candidate predictors, but multivariate statistical testing was not performed due to small sample size.

Results

Our patient cohort was composed of a heterogeneous population. Median patient age was 67.5 years (range 53–81). Twenty five percent of patients had prior thoracic radiation and 30% underwent prior thoracic surgery. The majority of patients had NSCLC (75%). Concurrent chemotherapy was given in 25% of patients, most commonly with carboplatin and paclitaxel regimen. Two patients were treated with 3DCRT, 4 IMRT/VMAT, 7 SBRT and 7 with proton RT. The median tumor EQD2 ($\alpha/\beta = 10$) was 77 Gy with a range of 59–126 Gy. The number of fractions ranged from 3 (SBRT) to 37 (conventional fractionation). Table 1 lists patient and treatment characteristics and subdivides individuals based on development of radiation pneumonitis. There were no significant differences between the two groups in regards to age, gender, histology, or treatment regimen/technique. However, the group sizes were unbalanced (4/20 patients developed grade ≥ 2 pneumonitis).

Functional lung dosimetry differed from anatomic lung dosimetry to varying degrees across the patient population. Figure 2 depicts radiation treatment plans from two patients with similar clinical characteristics but differences in mean dose to anatomic lung versus mean dose to perfused lung. Both patients presented with upper lobe primary NSCLC and were treated with conventionally fractionated concomitant radio-chemotherapy. One patient (B) underwent prior lobectomy greater than 1 year prior to receiving radio-chemotherapy for locoregionally recurrent tumor in the lung and nodes. The first patient (A) had a similar mean anatomic lung dose (MLD = 16.6 Gy = 13.6 Gy $EQD2_{lung}$) to the second patient (B, MLD = 16.4 Gy = 18.4 Gy $EQD2_{lung}$), yet developed radiation pneumonitis; however,

patient A had a higher dose to perfused lung regions ($pMLD_{70\%}$ = 24.2 Gy = 19.9 Gy $EQD2_{lung}$) than patient B ($pMLD_{70\%}$ = 8.6 Gy = 7.5 Gy $EQD2_{lung}$). This example highlights that solely using anatomic lung dose to predict risk of radiation pneumonitis may not be applicable for all patients, particularly those with spatial heterogeneity in lung function.

Neither dose-volume histograms (DVH) nor dose-function histograms (DFH) [6,20] could stratify patients for pneumonitis incidence risk. However, patients with pneumonitis tended to have higher doses to both anatomic lung and perfused lung. Figure 3 compares CT-based lung DVH (A) to MAA SPECT-based perfused lung DFH (B) for patients based on development of radiation pneumonitis (PMN+ versus PMN−). As revealed in these figures, there is no clear DVH or DFH threshold that completely separates patients based on pneumonitis status. However, the best separation emerges approximately in the range of $V_{15\text{-}25GyEQD2}$.

We performed operator characteristic (ROC) analysis showing areas under curve (AUC) as a function (Figure 4) incorporating dose-volume, dose-perfused volume, and mean perfused lung dose to identify candidate predictors of pneumonitis. Standard error bars in AUC estimates are displayed, with statistically significant parameter values shown in red (AUC > 0.93, $p < 0.01$). Statistically significant parameters with the smallest error in AUC were $V_{15GyEQD2}$, $V_{\text{-}40GyEQD2}$, MLD and $pMLD_{70\%}$. Cutoff values in parameters for maximum prediction accuracy of radiation pneumonitis were $V_{15GyEQD2}$ = 27.1% (100% sensitivity, 93.75% specificity, $p = 0.003$), MLD = 13.6 Gy $EQD2_{lung}$ (19.6 Gy for patients receiving 60 Gy in 30 fractions, 100% sensitivity, 93.75% specificity, $p = 0.006$), and $pMLD_{70\%}$ = 13.3 Gy $EQD2_{lung}$ (100% sensitivity, 81.25% specificity, $p = 0.008$).

The combination of an anatomic lung dosimetric parameter (MLD) and a functional lung dosimetric parameter ($pMLD_{70\%}$) may improve prediction accuracy of patients with ≥ grade 2 pneumonitis rather than using either parameter independently. Figure 5 illustrates this concept through a bivariate scatter plot of a functional dosimetric parameter ($pMLD_{70\%}$) vs. an anatomic dosimetric parameter (MLD) in Figure 5A or vs. a different anatomic dosimetric parameter ($V_{15GyEQD2}$) in Figure 5B for individual patients. Not all individuals with high anatomic lung dose went on to develop radiation pneumonitis, but those who also had high perfused lung dose all went on to develop radiation pneumonitis (black markers).

Our patient population showed a weak correlation between the statistically significant functional and anatomic lung dose parameters (i.e. $pMLD_{70\%}$ versus MLD, $pMLD_{70\%}$ versus $V_{15GyEQD2}$, etc., Spearman $R < 0.6$ for all comparisons), which was substantially lower than the expected correlation among anatomic lung dose parameters (i.e. MLD versus $V_{15GyEQD2}$, etc., Spearman $R > 0.9$ for all comparisons). Testing within a larger patient population may confirm certain parameter combinations as independent variables for multivariate prediction of pneumonitis.

Discussion

In current practice, radiation treatment planning does not take into account the regional variance in pulmonary function and its impact on relative risk of radiation-induced pulmonary toxicity. We developed a framework for investigating the association of baseline perfused lung dosimetry with incidence of symptomatic pneumonitis and applied it as a proof-of-principle to a patient cohort who underwent modern SPECT/CT image acquisition, reconstruction, and co-registration while in radiation treatment position. The framework enhanced the accuracy of the spatial alignment between perfused lung and radiation dose distributions, as compared to historical investigations. The preliminary application of the framework reveals that a combination of anatomic and functional lung dose parameters may be able to better predict patients who go on to present ≥ grade 2 radiation pneumonitis than either group of variables on their own.

Studies have looked at changes in pulmonary function tests following definitive radiotherapy for NSCLC. Schytte et al. [21] examined changes in PFTs following radiotherapy and noted association between V_{60Gy} and long-term changes in FEV1. Prior groups utilizing SPECT imaging for lung perfusion have not been able to define functional lung dosimetric parameters that can replace anatomic lung dosimetric parameter in predicting radiation pneumonitis. However, more recently, multiple groups have reported improved radiation pneumonitis correlation by utilizing baseline SPECT/CT lung perfusion imaging to define additional dosimetric parameters for treatment planning. Farr et al. [16] examined standard and functional DVH for patients with NSCLC treated with curative intent and noted functional dosimetric parameters had a stronger association of radiation pneumonitis than standard metrics. Additionally, supplementing standard metrics with functional parameters led to a higher sensitivity and specificity for radiation pneumonitis. Hoover et al. retrospectively reviewed SPECT/CT-based perfusion/ventilation lung parameters of patients undergoing thoracic radiotherapy, and their data suggested a higher sensitivity and specificity with perfused mean lung dose for radiation pneumonitis correlation (AUC = 0.81), compared to standard dose-volume constraints (AUC ≤ 0.73) [22]. Wang et al. echoes similar results, showing high correlation of perfusion metrics with radiation-induced lung injury and spatial differences between anatomic lung V_{60Gy} and perfused lung V_{60Gy} [23]. Recent data also showed that patients who had perfused-MLD > 16 Gy, perfused V_{20Gy} > 30%, and perfused V_{30Gy} > 23% went on to develop radiation pneumonitis [16]. Our data yielded similar mean dose to perfused lung as a predictor of pneumonitis, after accounting for differences in fractionation, regional lung dose variation, and statistical testing with multiple sampling correction to protect against false positive findings. Functional dosimetric parameters can complement anatomic parameters for improved correlation of pneumonitis.

In addition to investigations on baseline SPECT/CT imaging prior to radiation therapy [16,22,23], other studies have also correlated changes between pre- and post-treatment functional lung imaging and its relationship to radiation pneumonitis. Farr et al. noted a higher risk of symptomatic pneumonitis in those patients who had a reduction in perfusion at 3 months post-radiotherapy compared to patients who did not, with a relative risk estimate of 3.6 [24]. Although both perfusion and ventilation changes can be seen after treatment, ventilation metrics may not be as sensitive to radiation as perfusion metrics, since

physiologically, the lungs can vasoconstrict to reduce blood flow to unventilated areas, but it is more difficult to constrict airways to reduce ventilation to un-perfused areas [25]. Therefore, radiation-induced changes in ventilation will likely cause rapid changes in perfusion, but not vice versa.

Our methodological framework only utilized baseline perfusion imaging, which can determine pneumonitis risk *a priori* and inform on additional radiation planning lung constraints. A relationship likely exists for pre-treatment parameters and post-treatment changes; as in, high radiation dose to perfused lung will likely lead to greater reductions in lung perfusion post-treatment. This is consistent with findings from Farr et al., who found a greater risk of pneumonitis in patients who saw a greater reduction in perfusion [24]. If pre-treatment scans can be used to predict future development of pneumonitis, then treatment can potentially be adjusted to minimize risk of pulmonary toxicity. From this preliminary proof-of-principle investigation, a testable hypothesis would be that patients who have high anatomic mean lung dose can be risk stratified for the development of radiation pneumonitis by perfused mean lung dose. Validation of perfused lung dosimetric predictors in a future investigation would motivate the generation of functional lung avoidance treatment plans that are personalized to mitigated individual patient risk of pulmonary toxicity. Such conformal avoidance planning techniques of functional image-defined perfused lung tissue have been reported to be feasible [26–28].

This study has several limitations. The total number of patients evaluated is small with few events, which only permitted application of a methodological framework as a proof-of-principle. The preliminary results in this limited cohort confirm other studies on the potential utility regarding functional parameters predictive for pneumonitis. We have a heterogeneous patient population with respect to treatment modality and individual tumor characteristics. Some of our patients had prior radiation or thoracic surgery, albeit at long time intervals prior to treatment planning SPECT/CT imaging. Due to our small patient numbers, we were not able to perform subgroup analysis on the effect of prior therapy, but our baseline imaging studies and tests captured the pulmonary function status prior to the current course of radiation treatment. Despite these variations in patient characteristics, the observed trends support a testable hypothesis that functional and anatomic imaging parameters confer a substantial effect size for predicting radiation-induced pneumonitis.

The validity of the $EDQ2_{lung}$ voxelwise conversions for SBRT and moderately hypofractionated PBT is not precisely known, despite our efforts to control for treatment regimen and spatially variant lung fractional dose. Equivalent dose conversion for radiation toxicity prediction was carried out most recently by Chaudhuri et al [29] in patients who received SBRT, and their investigation reported increased risk of symptomatic pneumonitis for those who presented with higher pretreatment non-target lung FDG PET uptake and MLD > 5.9 Gy EQD2. Given that 70% of our patients were treated with either modality, our results should be interpreted with caution. In addition to dose, there are other known risk factors for pneumonitis, such as concurrent chemotherapy, prior radiotherapy, stage, tumor size, patient age, and comorbidities, which need to be considered. This initial application of our framework must be validated in a larger patient cohort.

Conclusions

This investigation demonstrated that construction of a comprehensive methodological framework can reveal differences between anatomic and perfused lung dosimetric parameters. The addition of perfused lung parameters may help to improve correlation to clinical radiation pneumonitis, especially for patient plans with high anatomic mean lung dose. Evaluation of anatomic and perfused lung dose parameters can further personalize radiation therapy planning to minimize risk of treatment-related toxicity.

Supplementary Material

Refer to Web version on PubMed Central for supplementary material.

Acknowledgments

This work was financially supported by NIH/NCI R01CA204301, Radiological Society of North America RSCH1405, and the Fred Hutchinson Cancer Center Support Grant for Protocol-Specific Research Support, P30CA015704. We express our gratitude to the Nuclear Medicine and Radiation Oncology staff for assisting with patient setup during all imaging scans.

References

1. Mehta V. Radiation pneumonitis and pulmonary fibrosis in non-small-cell lung cancer: pulmonary function, prediction, and prevention. Int J Radiat Oncol Biol Phys. 2005; 63:5–24. [PubMed: 15963660]
2. Palma DA, Senan S, Tsujino K, et al. Predicting radiation pneumonitis after chemoradiation therapy for lung cancer: an international individual patient data meta-analysis. Int J Radiat Oncol Biol Phys. 2013; 85:444–450. [PubMed: 22682812]
3. Marks LB, Bentzen SM, Deasy JO, et al. Radiation dose-volume effects in the lung. Int J Radiat Oncol Biol Phys. 2010; 76:S70–76. [PubMed: 20171521]
4. Graham MV, Purdy JA, Emami B, et al. Clinical dose-volume histogram analysis for pneumonitis after 3D treatment for non-small cell lung cancer (NSCLC). Int J Radiat Oncol Biol Phys. 1999; 45:323–329. [PubMed: 10487552]
5. Barriger RB, Fakiris AJ, Hanna N, Yu M, Mantravadi P, McGarry RC. Dose-volume analysis of radiation pneumonitis in non-small-cell lung cancer patients treated with concurrent cisplatinum and etoposide with or without consolidation docetaxel. Int J Radiat Oncol Biol Phys. 2010; 78:1381–1386. [PubMed: 20231061]
6. Marks LB, Spencer DP, Sherouse GW, et al. The role of three dimensional functional lung imaging in radiation treatment planning: the functional dose-volume histogram. Int J Radiat Oncol Biol Phys. 1995; 33:65–75. [PubMed: 7642433]
7. Evans ES, Hahn CA, Kocak Z, Zhou SM, Marks LB. The role of functional imaging in the diagnosis and management of late normal tissue injury. Semin Radiat Oncol. 2007; 17:72–80. [PubMed: 17395037]
8. Miften MM, Das SK, Su M, Marks LB. Incorporation of functional imaging data in the evaluation of dose distributions using the generalized concept of equivalent uniform dose. Phys Med Biol. 2004; 49:1711–1721. [PubMed: 15152926]
9. Seppenwoolde Y, Engelsman M, De Jaeger K, et al. Optimizing radiation treatment plans for lung cancer using lung perfusion information. Radiother Oncol. 2002; 63:165–177. [PubMed: 12063006]
10. Lind PA, Marks LB, Hollis D, et al. Receiver operating characteristic curves to assess predictors of radiation-induced symptomatic lung injury. Int J Radiat Oncol Biol Phys. 2002; 54:340–347. [PubMed: 12243806]

11. Petersson J, Sanchez-Crespo A, Larsson SA, Mure M. Physiological imaging of the lung: single-photon-emission computed tomography (SPECT). J Appl Physiol (1985). 2007; 102:468–476. [PubMed: 16990505]
12. Patton JA, Turkington TG. SPECT/CT physical principles and attenuation correction. J Nucl Med Technol. 2008; 36:1–10. [PubMed: 18287196]
13. Bailey DL, Willowson KP. Quantitative SPECT/CT: SPECT joins PET as a quantitative imaging modality. Eur J Nucl Med Mol Imaging. 2014; 41(Suppl 1):S17–25. [PubMed: 24037503]
14. Bailey DL, Willowson KP. An evidence-based review of quantitative SPECT imaging and potential clinical applications. J Nucl Med. 2013; 54:83–89. [PubMed: 23283563]
15. Mirnezami R, Nicholson J, Darzi A. Preparing for precision medicine. The New England journal of medicine. 2012; 366:489–491. [PubMed: 22256780]
16. Farr KP, Kallehauge JF, Moller DS, et al. Inclusion of functional information from perfusion SPECT improves predictive value of dose-volume parameters in lung toxicity outcome after radiotherapy for non-small cell lung cancer: A prospective study. Radiother Oncol. 2015; 117:9–16. [PubMed: 26303012]
17. Farr KP, Kramer S, Khalil AA, Morsing A, Grau C. Role of perfusion SPECT in prediction and measurement of pulmonary complications after radiotherapy for lung cancer. Eur J Nucl Med Mol Imaging. 2015; 42:1315–1324. [PubMed: 25862455]
18. Borst GR, Ishikawa M, Nijkamp J, et al. Radiation pneumonitis after hypofractionated radiotherapy: evaluation of the LQ(L) model and different dose parameters. Int J Radiat Oncol Biol Phys. 2010; 77:1596–1603. [PubMed: 20231066]
19. Benjamini Y, Hochberg Y. Controlling the False Discovery Rate - a Practical and Powerful Approach to Multiple Testing. J Roy Stat Soc B Met. 1995; 57:289–300.
20. Marks LB, Sherouse GW, Munley MT, Bentel GC, Spencer DP. Incorporation of functional status into dose-volume analysis. Medical physics. 1999; 26:196–199. [PubMed: 10076973]
21. Schytte T, Bentzen SM, Brink C, Hansen O. Changes in pulmonary function after definitive radiotherapy for NSCLC. Radiother Oncol. 2015; 117:23–28. [PubMed: 26455451]
22. Hoover DA, Reid RH, Wong E, et al. SPECT-based functional lung imaging for the prediction of radiation pneumonitis: a clinical and dosimetric correlation. J Med Imaging Radiat Oncol. 2014; 58:214–222. [PubMed: 24373453]
23. Wang D, Sun J, Zhu J, Li X, Zhen Y, Sui S. Functional dosimetric metrics for predicting radiation-induced lung injury in non-small cell lung cancer patients treated with chemoradiotherapy. Radiat Oncol. 2012; 7:69. [PubMed: 22594342]
24. Farr KP, Moller DS, Khalil AA, Kramer S, Morsing A, Grau C. Loss of lung function after chemo-radiotherapy for NSCLC measured by perfusion SPECT/CT: Correlation with radiation dose and clinical morbidity. Acta Oncol. 2015; 54:1350–1354. [PubMed: 26203930]
25. Robbins ME, Brunso-Bechtold JK, Peiffer AM, Tsien CI, Bailey JE, Marks LB. Imaging radiation-induced normal tissue injury. Radiat Res. 2012; 177:449–466. [PubMed: 22348250]
26. Siva S, Devereux T, Ball DL, et al. Ga-68 MAA Perfusion 4D-PET/CT Scanning Allows for Functional Lung Avoidance Using Conformal Radiation Therapy Planning. Technology in cancer research & treatment. 2016; 15:114–121. [PubMed: 25575575]
27. McGuire SM, Marks LB, Yin FF, Das SK. A methodology for selecting the beam arrangement to reduce the intensity-modulated radiation therapy (IMRT) dose to the SPECT-defined functioning lung. Phys Med Biol. 2010; 55:403–416. [PubMed: 20019404]
28. St-Hilaire J, Lavoie C, Dagnault A, et al. Functional avoidance of lung in plan optimization with an aperture-based inverse planning system. Radiother Oncol. 2011; 100:390–395. [PubMed: 21963286]
29. Chaudhuri AA, Binkley MS, Rigdon J, et al. Pre-treatment non-target lung FDG-PET uptake predicts symptomatic radiation pneumonitis following Stereotactic Ablative Radiotherapy (SABR). Radiother Oncol. 2016; 119:454–460. [PubMed: 27267049]

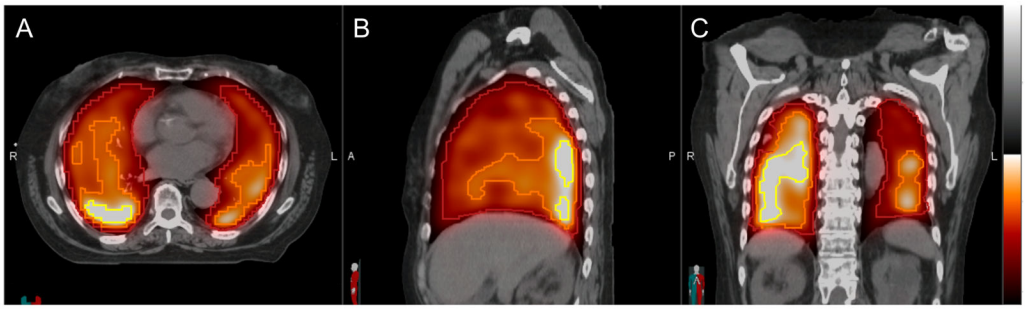

Figure 1. Functional lung threshold volumes defined on perfusion [^{99m}Tc]MAA SPECT fused to the planning CT (hot metal colorscale) in axial (A), sagittal (B), and coronal (C) planes

Example functional lung contours are shown that correspond to thresholds of >25% of maximum perfusion intensity within total lung minus GTV (pTL-GTV$_{25\%}$, dark red), >50% of maximum perfusion (pTL-GTV$_{50\%}$ orange), and >75% of maximum perfusion (pTL-GTV$_{75\%}$, yellow). Dosimetric parameters such as mean perfused lung dose were evaluated within threshold perfused lung volumes.

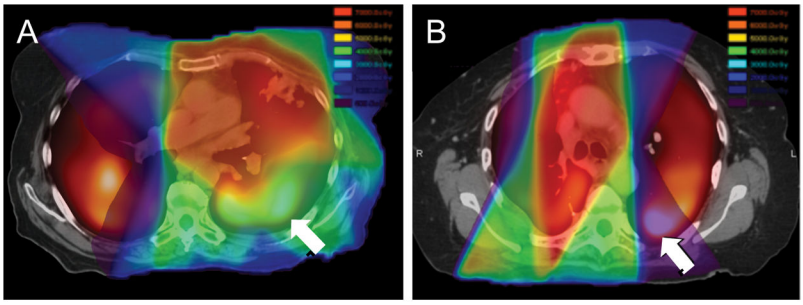

Figure 2. Planned dose (rainbow color scale) overlaid on fusion of MAA perfusion SPECT (hot metal color scale) and planning CT for patients with similar clinical characteristics (upper lobe tumors treated with concomitant radio-chemotherapy), one of whom presented with radiation pneumonitis (A) and the other who did not (B) after therapy

Arrows indicate high perfusion regions and their spatial relationship to the local dose distribution.

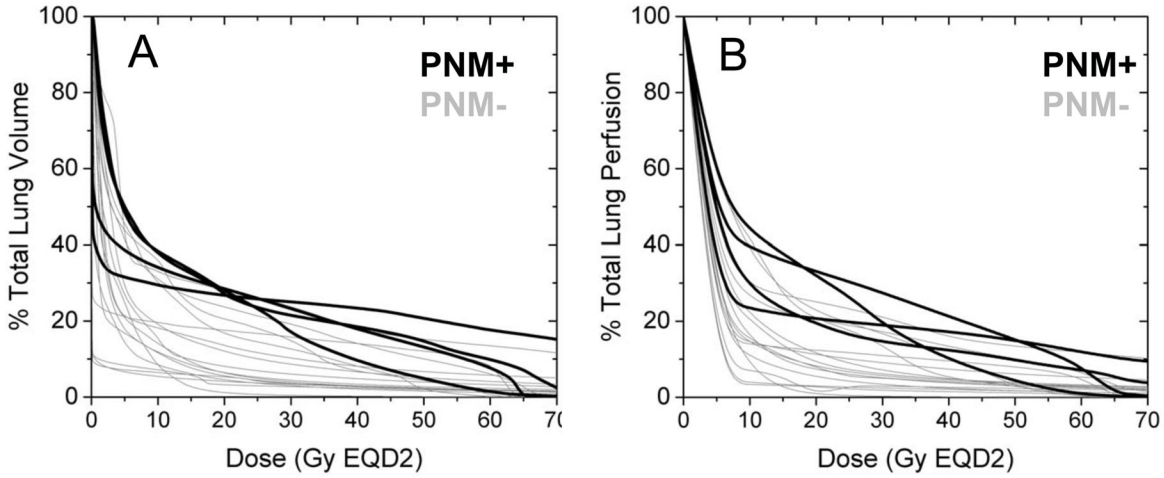

Figure 3. CT-based total lung dose-volume histogram (A) and MAA SPECT-based perfused lung dose-function histogram (B) for the cohort of lung cancer patients

Patient DVH and DFH are color-coded according to those who presented with (black lines) or without (gray lines) grade 2 or higher pneumonitis after radiation therapy.

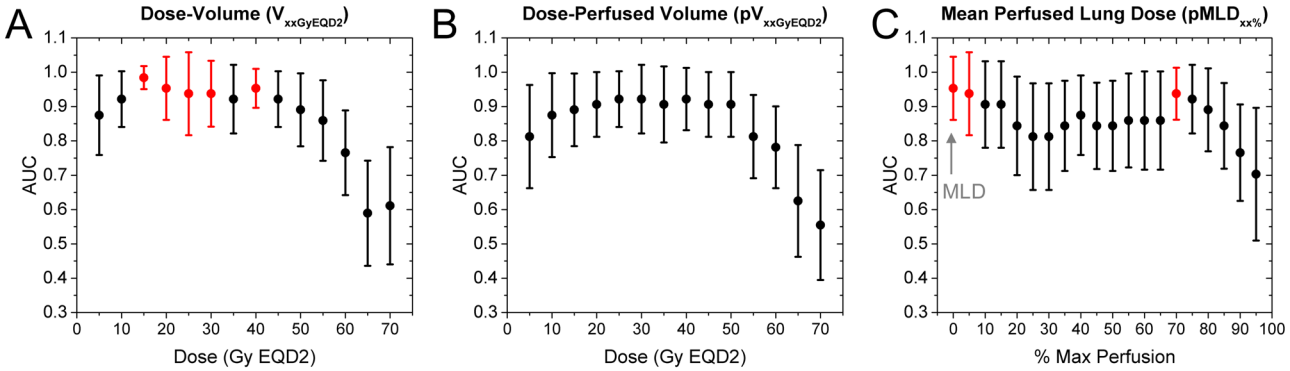

Figure 4. Receiver operator characteristic (ROC) analysis showing areas under curve (AUC) as a function of dose-volume parameters (A), dose-perfused volume parameters (B), and mean perfused lung dose parameters (C)

Red markers (AUC > 0.93, $p < 0.01$) signify candidate predictors of grade 2 or higher pneumonitis, including $V_{15GyEQD2}$, mean lung dose (MLD), and mean perfused lung dose above 70% max perfusion threshold ($pMLD_{70\%}$). Standard error bars in AUC are displayed.

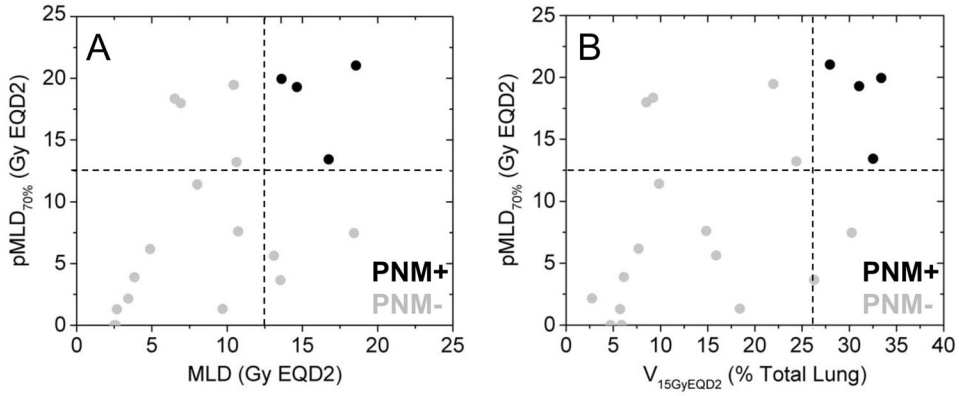

Figure 5. Bivariate scatter plot as a function of patients who presented with (black markers) or without (gray markers) grade 2 or higher pneumonitis after radiation therapy

(A) mean perfused lung dose above 70% max perfusion threshold ($pMLD_{70\%}$) vs. mean lung dose (MLD), and (B) $pMLD_{70\%}$ vs $V_{15GyEQD2}$. Dashed lines are representative bivariate thresholds in each parameter that yields perfect separation.

Table I

Patient characteristics

Characteristic	N (%)	Without G2+ pneumonitis (N=16)	With G2+ pneumonitis (N=4)
Age at time of radiation treatment (years)	Median: 67.5 Range: 53–81	Median: 66.5 Range: 55–81	Median: 75 Range: 53–78
Sex			
Male	9 (45)	7	2
Female	11 (55)	9	2
Clinical Stage			
Limited stage (III) SCLC	2 (10)	2	0
I NSCLC	2 (10)	2	0
II NSCLC	3 (15)	2	1
IIIA NSCLC	3 (15)	2	1
IIIB NSCLC	2 (10)	1	1
Locally Recurrent	5 (25)	4	1
Metastatic to Lung	3 (15)	3	0
Histology			
NSCLC	15 (75)	11	4
SCLC	2 (10)	2	0
Other (other primary)	3 (15)	3	0
Prior thoracic radiation			
Yes	5 (25)	5	0
No	15 (75)	11	4
Prior thoracic surgery			
Yes	6 (30)	4	2
No	14 (70)	12	2
Concurrent chemotherapy			
Yes	5 (25)	2	3
No	15 (75)	14	1
EQD2 Radiation dose (Gy)	Median: 76.78 Range: 59–126	Median: 70 Range: 59–126	Median: 66.3 Range: 65.5–70
Radiation treatment technique			
3D CRT	2	2	0
IMRT/VMAT	4	2	2
SBRT	7	7	0
PBT	7	5	2
Smoking status			
lifetime nonsmoker	3	3	0
former	14	10	4
current	3	3	0
Pre-existing COPD			
Yes	11	9	2
No	9	7	2